

Growing Perfect Single-Crystal Epitaxial Films of $(\text{Si}_2)_{1-x}(\text{GaN})_x$ Solid Solutions on Si (111) Substrates from the Liquid Phase

A.S. SAIDOV^a, SH.N. USMONOV^a, M.U. KALANOV^b,
D.V. SAPAROV^{a,*}, T.T. ISHNIYAZOV^a, A.M. AKHMEDOV^c,
M.B. TAGAEV^d AND A.SH. RAZZOKOV^e

^aPhysical–Technical Institute, Uzbekistan Academy of Sciences, 2B Ch. Aytmatov St., 100084 Tashkent, Uzbekistan

^bInstitute of Nuclear Physics, Uzbekistan Academy of Sciences, 1 Khurasan St., 100214 Tashkent, Uzbekistan

^cTashkent Institute of Irrigation and Agricultural Mechanization Engineers, 39 Kori Niyoziy St., 100084 Tashkent, Uzbekistan

^dKarakalpak State University named after Berdak, 1 Ch. Abdirov St., 230112 Nukus, Republic of Karakalpakstan, Uzbekistan

^eUrgench State University, 14 Kh. Alimdjan St., 220100 Urgench City, Uzbekistan

Received: 07.02.2025 & Accepted: 16.07.2025

Doi: [10.12693/APhysPolA.148.29](https://doi.org/10.12693/APhysPolA.148.29)

*e-mail: dada@uzsci.net

The technological capabilities of the method of liquid-phase epitaxy from a limited volume of Sn solution-melt for obtaining films of substitutional solid solution $(\text{Si}_2)_{1-x}(\text{GaN})_x$ on Si (111) substrates are shown. The grown films had a single-crystal structure with (111) orientation, n-type conductivity with a resistivity of $\rho \simeq 1.38 \, \Omega \, \text{cm}$, a carrier concentration of $n \simeq 3.4 \times 10^{16} \, \text{cm}^{-3}$, and a charge carrier mobility of $\mu \simeq 133 \, \text{cm}^2/(\text{V} \, \text{s})$. The relatively narrow width (full width at half maximum of 780 arcsec) and high intensity (2×10^5 pulses/s) of the main structural reflection $(111)_{\text{Si/GaN}}$ indicate a high degree of perfection of the crystal lattice of the epitaxial layer $(\text{Si}_2)_{1-x}(\text{GaN})_x$. The photosensitivity region of p-Si-n- $(\text{Si}_2)_{1-x}(\text{GaN})_x$ heterostructures covers the photon energy range from 1.2 to 2.4 eV, with a maximum at 1.9 eV.

topics: epitaxial film, X-ray diffraction analysis, spectral photosensitivity

1. Introduction

Growing the epitaxial layers of perspective and popular semiconductor materials on silicon substrates is becoming relevant to reduce the cost of the final product and to integrate existing silicon technology with the technology of III–V and II–VI binary compounds [1–4]. One of the promising directions in this area is the growth of epitaxial films of popular semiconductors, such as GaN, SiC, GaAs, and InP, on silicon substrates. In the production of semiconductor devices, manufacturing costs are almost independent of the diameter of the substrate material. On the other hand, when using substrates of larger diameter, the number of devices made from them is significantly greater than when substrates of smaller diameter are used, which makes it possible to reduce the cost of the final product several times. Today, high-quality Si substrates with large diameters are available, reaching up to 200 mm or

even up to 300 mm. Therefore, a lot of research is being carried out on growing epitaxial films of expensive and in-demand semiconductors on cheap Si substrates.

However, when growing epitaxial films on foreign substrates of large diameter, problems arise associated with the bending of the substrates and the occurrence of defects in the epitaxial film. This is due to the difference in the lattice constants and thermal expansion coefficients of the materials of the grown epitaxial layer and substrate. In order to use epitaxial films grown on foreign substrates in production lines, according to modern technical requirements, the bending of the substrate should not exceed a certain value. For example, according to SEMI M1-0600 standards, the bending value of a substrate with a diameter of 150 mm should not exceed $60 \, \mu\text{m}$ [5].

The bending of the fabricated structure depends on: Young's modulus of the substrate (E_{sub}) and the film (E_{epi}), the thickness of the substrate (t_{sub})

and the film (t_{epi}), the thermal expansion coefficient of the substrate (α_{sub}) and the film (α_{epi}), the diameter of the substrate (d), and the difference between the growth temperatures and room temperature (ΔT) [6]. This can be written as

$$Bow = -\frac{3}{4} \frac{E_{\text{epi}}}{E_{\text{sub}}} \frac{t_{\text{epi}}}{t_{\text{sub}}^2} (\alpha_{\text{sub}} - \alpha_{\text{epi}}) d^2 \Delta T. \quad (1)$$

As seen from (1), there is a quadratic dependence of the bending of the resulting epitaxial film on the substrate diameter. On the other hand, the quality of the epitaxial film depends on the value of the bend. According to G.G. Stoney's equation, the smaller the bending of the resulting heterostructure, the lower the mechanical stress in the epitaxial film and the better the film quality [7]. Thus,

$$\sigma = \frac{E t^2}{6 f} \left(\frac{1}{R_2} - \frac{1}{R_1} \right), \quad (2)$$

where σ is the average value of mechanical stress in the epitaxial film, t is the substrate thickness, E is the biaxial module, the value of which for the silicon substrate is 203 GPa, R_1 is radius of curvature of the sample before epitaxy, R_2 is the radius of curvature of the sample after deposition of the epitaxial film, and f is the thickness of the epitaxial film.

Various methods are used to reduce the bending of the fabricated heterostructure as well as to improve the quality of the epitaxial film. For example, when producing a GaN epitaxial layer on Si substrates, various buffer layers are used between the substrate and the epitaxial film, which contribute to the production of higher-quality GaN epitaxial layers. In works [8–10], the possibility of reducing the bending of an epitaxial film and obtaining high-quality GaN layers by epitaxy from metal–organic compounds on Si (111) substrates by using AlN and AlGaN buffer layers was reported.

In this work, we investigated the possibility of growing graded-gap epitaxial layers of the $(\text{Si}_2)_{1-x}(\text{GaN})_x$ solid solution on Si substrates from the liquid phase, which can be used as a buffer layer to obtain high-quality GaN epitaxial layers on Si substrates.

2. Materials and methods

Layers of $(\text{Si}_2)_{1-x}(\text{GaN})_x$ solid solutions were grown on Si (111) substrates by liquid-phase epitaxy from a limited volume of Sn solution-melt in a vertical-type quartz reactor with horizontally located substrates using the technology described in [11, 12]. The substrates were separated from each other vertically by graphite supports. Thus, a limited gap was formed between the substrates, into which the solution-melt was poured. The distance between the substrates, i.e., the thickness of the solution-melt, was varied from 0.5 to 2.5 mm by selecting the thickness of the supports. The substrates were mounted on a cassette made of extremely pure

graphite. Several (up to ten) substrates could be placed in the cassette. The cassette had a cylindrical shape with three slots on the side. The slots in the cassette were intended for pouring the solution-melt into the gap between the substrates. The washer-shaped silicon substrates had a diameter of 20 mm, a thickness of 400 μm , crystallographic orientation (111), and p-type conductivity with a resistivity of 0.01 $\Omega \text{ cm}$ and were doped with B. The solution-melt was located in a quartz crucible, and the crucible was placed at the bottom of the reactor, 3–4 cm below the cassette. To prevent uncontrolled impurities from entering the reactor, the film growth process was carried out in a flow of pure hydrogen. Hydrogen purification was performed using a palladium filter. After placing the cassette (with the substrates) and the crucible (with the solution-melt) into the reactor, the entire system was pumped out to a vacuum level of 10^{-2} Pa and then purged with hydrogen for 15 min. After this, the heating of the reactor began. The cassette and crucible were in the isothermal zone of the reactor. To obtain a homogeneous solution-melt, the crucible temperature was kept for 30 min at 10 degrees higher than the temperature at which crystallization of the epitaxial film began. When the required temperature was reached (the beginning of crystallization), the cassette with the substrates was dipped into the solution-melt to fill the gaps between the substrates with the solution-melt. Then the cassette was raised 3–4 cm above the crucible. After this, the process of forced cooling of the reactor was carried out at a given speed. When the solution-melt was cooled, the crystallization of the epitaxial layer began. The crystallization process was carried out at different cooling rates, ranging from 0.5 to 2 degrees per minute. The set cooling rate was maintained automatically. An important aspect of liquid-phase epitaxy is the timely stopping of layer growth and removal of the remaining solution-melt from the surface of the films. In fact, crystallization of the epitaxial layer continued until the remaining solution-melt was removed from the gap between the substrates. The solution-melt was drained, and its residues were removed from the surface of the films by rapidly rotating the cassette (at a speed of 2500 rpm) with an electric motor. When the cassette rotates, due to centrifugal force, the surface of the epitaxial films is completely cleared of the remnants of the solution-melt.

An important factor in the process of epitaxial growth of a $(\text{Si}_2)_{1-x}(\text{GaN})_x$ solid solution from the liquid phase is the saturation of the solution-melt with Si_2 and GaN molecules and not with the individual Si, Ga, and N atoms at a given temperature. For this purpose, the solubility of Si and GaN in Sn was studied. It should be noted that the melting point of GaN is 2500°C. When GaN is dissolved in Sn at 980°C (below the melting point), the GaN is in the solution-melt in the form of Ga–N molecules (Fig. 1) and does not decompose

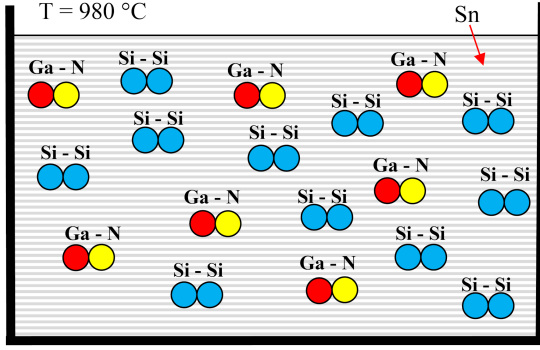


Fig. 1. Dissolution of the binary compound GaN and Si in the form of Ga-N and Si_2 molecules in Sn at 980°C (limited solubility).

into individual Ga and N atoms, similar to the way GaAs and ZnSe molecules in the Sn melt do not decompose into individual atoms of Ga, As, Zn, and Se at 750°C [13].

This statement is justified by the fact that the solubility of GaN in metals, in particular in Sn, is very small and amounts to ~ 0.002 mol.% at 1500°C. If GaN molecules were to decompose into the individual Ga and N atoms, the solubility of GaN in Sn would be unlimited, since from the phase diagram of the Ga-Sn binary alloy, it follows that the solubility of Ga in Sn is unlimited [14]. At this temperature, N is in a gaseous state and completely evaporates into the atmosphere (the dissolution of GaN in Sn is carried out in an open system, in a stream of purified H_2). Based on this, we can conclude that when GaN is dissolved in Sn at 980°C, it is in the solution-melt form of Ga-N molecules and does not decompose into individual Ga and N atoms.

The structural features of the grown epitaxial GaN films were studied using a DRON-3M X-ray diffractometer ($\text{Cu } K_\alpha$, $\lambda = 0.15418$ nm) according to the θ - 2θ scheme in step-by-step scanning mode. The dependence of the photosensitivity of the p-Si-n- $(\text{Si}_2)_{1-x}(\text{GaN})_x$ structure on photon energy was also studied. Photosensitivity in this case means the short-circuit current of the structure, normalized to a single photon.

3. Results and discussion

Epitaxial films of the $(\text{Si}_2)_{1-x}(\text{GaN})_x$ solid solution were grown at different values of the following technological process parameters: crystallization beginning and end temperatures, composition, thickness, and cooling rates of the solution-melt. The highest-quality films were grown at crystallization beginning and end temperatures of 980°C and 880°C, respectively, with a thickness and cooling rate of the solution-melt of 1 mm and 1 deg/min, respectively.

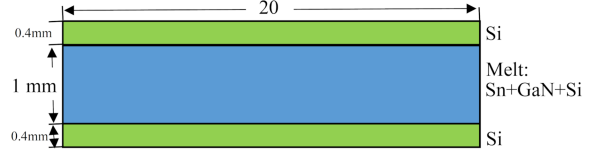


Fig. 2. Scheme of growing epitaxial films of solid solution $(\text{Si}_2)_{1-x}(\text{GaN})_x$ from a solution-melt consisting of Sn + GaN + Si on Si substrates.

Figure 2 shows the scheme of growing epitaxial films of the solid solution $(\text{Si}_2)_{1-x}(\text{GaN})_x$ from a solution-melt consisting of Sn + GaN + Si on Si substrates. The diameter and thickness of the Si substrates are 20 mm and 400 μm , respectively. The thickness of the solution-melt located between the horizontally positioned Si substrates is 1 mm. When the solution-melt is cooled from 980 to 880°C, an epitaxial layer of the solid solution $(\text{Si}_2)_{1-x}(\text{GaN})_x$ of ~ 10 μm thickness is grown on the Si substrates. Composition of the solution-melt was as follows: Sn — 200 g, GaN — 360 mg, and Si — 2.8 g.

Since the growth of the $(\text{Si}_2)_{1-x}(\text{GaN})_x$ solid solution was carried out from a limited volume of the solution-melt, the composition of the grown epitaxial film changes smoothly in the growth direction from Si to GaN. This helps to level out the mismatch between the lattice constants and thermal expansion coefficients of the silicon substrate and the epitaxial film, which in turn helps to obtain higher-quality GaN films on the surface of the Si substrate.

The thickness of the grown epitaxial films was ~ 10 μm . The specially undoped films of the $(\text{Si}_2)_{1-x}(\text{GaN})_x$ solid solution had n-type conductivity with a resistivity of $\rho \simeq 1.38$ Ω cm; the concentration and mobility of charge carriers at 300 K are $n \simeq 3.4 \times 10^{16}$ cm^{-3} and $\mu \simeq 133$ $\text{cm}^2/(\text{V s})$, respectively.

Figure 3 shows a diffraction pattern of the grown epitaxial film of the $(\text{Si}_2)_{1-x}(\text{GaN})_x$ solid solution. Analysis of the diffraction pattern showed that it contains several selective structural reflections with different intensities and one diffuse reflection at small scattering angles. The most intensive main reflection $(111)_{\text{Si/GaN}}$ at $2\theta = 28.33^\circ$ is due to the atomic planes of the silicon lattice with the (111) orientation; its beta (β) component is visible at $2\theta = 25.73^\circ$. The second $((222)_{\text{Si/GaN}})$ and third $((333)_{\text{Si/GaN}})$ orders of the main reflection are observed at scattering angles $2\theta = 58.65^\circ$ and $2\theta = 94.70^\circ$, respectively. The diffraction pattern near the main reflection also contains narrow structural reflections with low intensity, caused by the reflection from the structural phases of cubic modification gallium nitride (c-GaN) $((111)_{\text{GaN(c)}})$ with the (111) orientation and $d/n = 0.2599$ nm at $2\theta = 34.4^\circ$ and hexagonal modification of (h-GaN) $((002)_{\text{GaN(h)}})$ with (002)

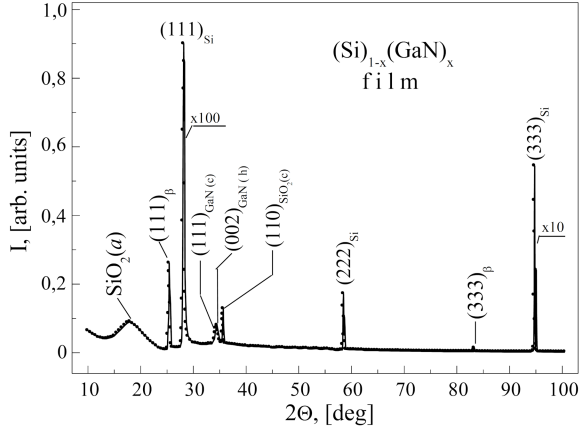


Fig. 3. X-ray diffraction pattern of $(\text{Si}_2)_{1-x}(\text{GaN})_x$ solid solution films.

orientation and $d/n = 0.2592$ nm at $2\theta = 34.6^\circ$. The wide diffuse reflection observed at $2\theta \approx 16.8^\circ$ with $d/n = 0.6061$ nm is due to structural fragments of quartzite SiO_2 with a size of $L_d \approx 1$ nm in the amorphous phase ($\text{SiO}_2(a)$), which are located on the surface layers of the film. The narrow width of the main reflection $(111)_{\text{Si/GaN}}$ with full width at half maximum (FWHM) of 780 arcsec and its high intensity (2×10^5 pulses/sec), as well as the presence of selective structural reflections of the (hhh) -type in the diffraction pattern (where $h = 1, 2$, and 3) indicate that the film has a perfect single-crystal structure with crystallographic orientation (111). The sizes of sub-crystallites were estimated using the Selyakov–Scherrer method based on the half-width of the main reflection [15], which is ~ 40 nm. It should also be noted that the value of FWHM = 780 arcsec of the main reflection of $(111)_{\text{Si/GaN}}$ is comparable with the best results of other authors (FWHM = 790 arcsec of (0002) [7] and FWHM = 782.28 arcsec of (0002) [10]). The authors of the mentioned works showed that the smaller the peak half-width (FWHM) of the rocking curve, the smaller the bending of the GaN epitaxial film grown on a Si substrate. The minimum FWHM values of 780–790 arcsec were obtained for epitaxial GaN films grown through AlGaIn buffer layers.

The appearance of reflections of the second $(222)_{\text{Si/GaN}}$ and third $(333)_{\text{Si/GaN}}$ order in the diffraction pattern, as well as the weak splitting of the main reflection into α_1 and α_2 components of radiation with intensities $I_{(111)}(\alpha_1) \neq 2I_{(111)}(\alpha_2)$, indicates the existence of the elastic micro-stresses of a growth nature in the lattice of the epitaxial film. However, the complete splitting of the third-order reflection is observed with the radiation intensity ratio close to the theoretical value — $I_{(333)}(\alpha_1) \approx 2I_{(333)}(\alpha_2)$. This indicates that the elastic micro-stresses are concentrated in the near-surface layer of the crystal lattice of the epitaxial film. The elastic micro-stresses of a growth nature are apparently

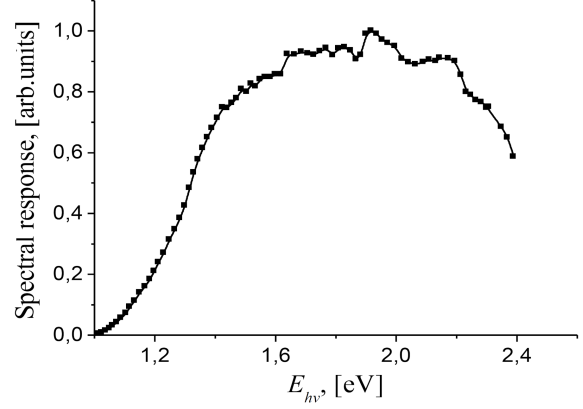


Fig. 4. Dependence of the photosensitivity of p-Si-n- $(\text{Si}_2)_{1-x}(\text{GaN})_x$.

caused by the difference in the ionic radii of gallium ($r_{\text{Ga}^{3+}} = 0.062$ nm), nitrogen ($r_{\text{N}^{3-}} = 0.146$ nm), and silicon ($r_{\text{Si}^{4+}} = 0.040$ nm), which are located at the sites of the crystal lattice of the $(\text{Si}_2)_{1-x}(\text{GaN})_x$ solid solution [16, 17].

To minimize the energy of elastic distortions, nanocrystallites of the c-GaN and h-GaN gallium nitride phases with sizes of $L_{\text{GaN}} \approx 47$ nm appeared in the crystal lattice. They contribute to the “relaxation” of the crystal lattice. Reflections of these phases have a noticeable intensity and a narrow width of 3.2×10^{-3} rad. The low-angle arrangement of the $(111)_{\text{GaN}(c)}$ and $(002)_{\text{GaN}(h)}$ reflections indicates that the c-GaN and h-GaN nanocrystallites are located in the surface layer of the film, and they are coherently located in the lattice of the solid solution.

Figure 4 shows the dependence of the photosensitivity of the fabricated p-Si-n- $(\text{Si}_2)_{1-x}(\text{GaN})_x$ structures. As can be seen in the figure, the increase in the photosensitivity of the p-Si-n- $(\text{Si}_2)_{1-x}(\text{GaN})_x$ heterostructure begins with a photon energy of ~ 1.1 eV, which is associated with silicon (with a band gap $(E_g)_{\text{Si}} = 1.1$ eV), and the photosensitivity region expands towards short waves of the electromagnetic radiation spectrum, which shows the influence of the wide-band component of the solid solution — GaN (with a band gap $(E_g)_{\text{GaN}} = 3.4$ eV) — in the photo-voltaic process. The maximum photosensitivity is achieved at photon energies $E_{h\nu} = 1.9$ eV. In addition, at $E_{h\nu} = 1.62$ eV, the second rise is observed in the 1.65–1.86 eV range of the shelf, and at energies of 1.92, 2.17, and 2.3 eV, maxima are observed. Such a complex character of the spectral dependence of the photosensitivity of the studied structure is apparently due to the heterogeneity of the composition of the graded-gap epitaxial layer of the n- $(\text{Si}_2)_{1-x}(\text{GaN})_x$ solid solution. Each sublayer is enriched with silicon or gallium nitride, and nanocrystallites of the c-GaN and h-GaN

modifications present in the near-surface layer of the solid solution contribute to the photogeneration of nonequilibrium charge carriers and, consequently, to the creation of the photocurrent of the studied structure. According to X-ray structural analysis, the GaN content in the near-surface region of the epitaxial layer of the $(\text{Si}_2)_{1-x}(\text{GaN})_x$ solid solution is ~ 85 mol.%, i.e., $x = 0.85$.

4. Conclusions

Thus, the possibility of the growth of substitutional solid solutions $(\text{Si}_2)_{1-x}(\text{GaN})_x$ from a limited volume of Sn solution-melt on Si (111) substrates has been investigated. It was demonstrated that when dissolved in Sn at 980°C , GaN is in the form of Ga–N molecules and does not decompose into the individual Ga and N atoms. Grown films had n -type conductivity. X-ray diffraction analysis showed that the grown epitaxial film has a single-crystal structure with (111) orientation. The relatively narrow width (FWHM = 780 arcsec) and high intensity (2×10^5 impulse/s) of the main reflection (111)_{Si/GaN} indicate a high degree of perfection of the crystal lattice of the epitaxial layer of the $(\text{Si}_2)_{1-x}(\text{GaN})_x$. In the near-surface region of the epitaxial film, coherently located nanocrystallites of the cubic (c-GaN) and hexagonal (h-GaN) phases of gallium nitride are formed. According to X-ray structural analysis, the GaN content in the near-surface region of the epitaxial layer of the $(\text{Si}_2)_{1-x}(\text{GaN})_x$ solid solution is ~ 85 mol.%, i.e., $x = 0.85$. The spectral photosensitivity region of p-Si–n- $(\text{Si}_2)_{1-x}(\text{GaN})_x$ structures covers the photon energy range from 1.2 to 2.4 eV with a maximum at 1.9 eV, which is of interest for the development of optoelectronic devices operating in the visible region of the radiation spectrum.

Acknowledgments

This work was financially supported by the Fundamental Research Programs of the Uzbekistan Academy of Sciences.

References

- [1] M.A. Fakhri, A.A. Alwahib, E.T. Salim et al., *Silicon* **15**, 7523 (2023).
- [2] L. Ravi, M.A. Rather, K.-L. Lin, C.-T. Wu, T.-Y. Yu, K.-Y. Lai, J.-I. Chyi, *ACS Appl. Electron. Mater.* **5**, 146-154 (2023).
- [3] H.D. Jabbar, M.A. Fakhri, M.J. AbdulRazaq, *Silicon* **14**, 12837 (2022).
- [4] Danmei Zhao and Degang Zhao, *J. Semicond.* **39**, 033006 (2018).
- [5] L. Wang, G. Walker, J. Chai, A. Iacopi, A. Fernandes, S. Dimitrijevic, *Sci. Rep.* **5**, 15423 (2015).
- [6] H. Aida, H. Takeda, N. Aota, K. Koyama, *Jpn. J. Appl. Phys.* **51**, 016504 (2012).
- [7] K. Cheng, M. Leys, S. Degroote, B. Van Daele, S. Boeykens, J. Derluyn, M. Germain, G. Van Tendeloo, J. Engelen, G. Borghs, *J. Electron. Mater.* **35**, 592 (2006).
- [8] J.H. Lee, K.S. Im, *Crystals* **11**, 234 (2021).
- [9] A. Able, W. Wegscheider, K. Engl, J. Zweck, *J. Cryst. Growth* **276**, 415 (2005).
- [10] M. Mansor, R. Norhaniza, A. Shuhaimi, M.I. Hisyam, A. Omar, A. Williams, M.R.M. Hussin, *Sci. Rep.* **13**, 8793 (2023).
- [11] A.S. Saidov, Sh.N. Usmonov, D.V. Saparov, *Adv. Mater. Sci. Eng.* **2019**, 3932195 (2019).
- [12] A.S. Saidov, D.V. Saparov, S.N. Usmonov, A.S. Razzakov, M. Kalanov, *Int. J. Mod. Phys. B* **37**, 2350132 (2022).
- [13] A.S. Saidov, D.V. Saparov, S.N. Usmonov, K.G. Gaimnazarov, I.I. Maripov, *IOP Conf. Ser. Mater. Sci. Eng.* **1181** 012002 (2022).
- [14] D. Zivkovic, D. Manasijevic, Z. Zivkovic, *J. Therm. Anal. Calorim.* **74**, 85 (2003).
- [15] A.A. Rusakov, *X-Ray Radiography of Metals*, Atomizdat, Moscow 1977 (in Russian).
- [16] I.L. Shul'pina, R.N. Kyutt, V.V. Ratnikov, I.A. Prokhorov, I.Z. Bezbakh, M.P. Shcheglov, *Tech. Phys.* **55**, 537 (2010).
- [17] V.K. Kiselev, S.V. Obolenskii, V.D. Skupov, *Tech. Phys.* **44**, 724-725 (1999).